Geomechanics and Engineering, *Vol. 24, No. 2 (2021) 193-203*
DOI: https://doi.org/10.12989/gae.2021.24.2.193

Influence of soil model complexity on the seismic response of shallow foundations

Saif Alzabeebee*

Department of Roads and Transport Engineering, College of Engineering, University of Al-Qadisiyah, Al-Qadisiyah, Iraq

(Received June 15, 2020, Revised January 8, 2021, Accepted January 13, 2021)

Abstract. The time-history finite element analysis is usually used to evaluate the seismic response of shallow foundations. However, the literature lacks studies on the influence of the soil constitutive model complexity on the seismic response of shallow foundations. This study, thus, aims to fill this gap by investigating the seismic response of shallow foundation resting on dry silica sand using the linear elastic (LE) model, elastic-perfectly-plastic (EPP) model, and hardening soil with small strain stiffness (HS small) model. These models have been used because it is intended to compare the results of a soil constitutive model that accurately captures the seismic response of the soil-structure interaction problems (which is the HS small model) with simpler models (the LE and EPP models) that are routinely used by practitioners in geotechnical designs. The results showed that the LE model produces a very small seismic settlement value which is approximately equal to zero. The EPP model predicts a seismic settlement higher than that produced using the HS small model for earthquakes with a peak ground acceleration (PGA) lower than 0.25 g for a relative density of 45% and 0.40 g for a relative density of 70%. However, the HS small model predicts a seismic settlement higher than the EPP model beyond the aforementioned PGA values with the difference between both models increases as the PGA rises. The results also showed that the LE and EPP models predict similar trend and magnitude of the acceleration-time relationship directly below the foundation, which was different than that predicted using the HS small model. The results reported in this paper provide a useful benchmark for future numerical studies on the response of shallow foundations subjected to seismic shake.

Keywords: soil constitutive model; finite element analysis; earthquake effect; shallow foundation

1. Introduction

The seismic soil-structure interaction problems are usually evaluated using the time-history finite element analysis due to the complexity of the earthquake effect (Kontoe *et al.* 2011, Yeganeh and Fatahi 2019, Alzabeebee 2020a). The use of the finite element method to model soil-structure interaction problems requires the utilization of a constitutive relationship to simulate the response of the soil and the structure. Furthermore, an advanced soil constitutive relationship (soil model) that robustly models the behaviour of soil response under seismic condition is required for accurate modelling of the seismic soil-structure interaction problems. However, the parameters for advanced soil models are not readily available, which makes the use of such models challenging (Brinkgreve *et al.* 2010). In addition, the advanced soil models require more computational time, which also adds to the justification of using simple soil models. More importantly, not all finite element packages have these models already implemented (Kontoe *et al*. 2011). These challenges made the use of simple models such as the linear elastic soil (LE) model and the elastic-perfectly-plastic soil model (EPP) more popular in practice and research (Kontoe *et al*. 2011, Kampas *et al.* 2018). The Rayleigh damping are usually used with these simple soil models to compensate the lack of hysteresis damping (Kontoe *et al.* 2011). However, it is worthy to state that these simple soil models do not account to the effect of the small strain stiffness, cyclic loads, hysteretic damping, and stiffness degradation (Alzabeebee 2019a).

As the LE and EPP soil models are preferred in practice, it is necessary to compare the results of the seismic soil-structure interaction using these simple models with the results of a verified soil model that can accurately model the seismic soil-structure interaction problems. This is very important to understand the influence of selecting the soil constitutive model on the results of the seismic soil-structure interaction problems. These comparisons also enable understanding the consequences of neglecting the effect of the small strain stiffness, cyclic loads, hysteretic damping, and stiffness degradation on the accuracy of the finite element analysis. However, there is lack of studies on the impact of the sophistication of the soil constitutive relationship on the outcomes of the seismic soil-structure interaction simulation as there are only three studies concerned with this topic. These previous studies focused only on the case of a tunnel buried in a clayey soil (Kontoe *et al*. 2011), a tunnel buried in a granular soil (Kampas *et al*. 2018), and a multistory building resting on a clayey sand (Yeganeh and Fatahi 2019). Hence, there are still gaps in knowledge regarding the effect of the complexity of soil constitutive model on the behaviour of shallow foundations

*Corresponding author, Ph.D.
E-mail: Saif.Alzabeebee@gmail.com,
Saif.Alzabeebee@qu.edu.iq

ISSN: 2005-307X (Print), 2092-6219 (Online)

resting on cohesionless soils as no efforts have been given in the literature to this important geotechnical problem. This study, therefore, aims to provide a comprehensive insight into the effect of the soil constitutive model on the seismic response of shallow foundation by comparing the results of the soil models which cannot capture the actual response of the soil under dynamic loads (namely the LE model and the EPP model) with the hardening soil with small strain stiffness model, which is a robust soil constitutive model with very good potentials to simulates the response of dry cohesionless soils subjected to seismic loads. The verification of the capabilities of the hardening small strain stiffness soil model to simulate the response of the soil-structure interaction problems under the effect of the seismic events has been reported by many studies in the literature (e.g., Al-Defae *et al*. 2013, Amorosi *et al*. 2014, Liang *et al*. 2015, Knappett *et al*. 2015, Fabozzi and Bilotta 2016, Amorosi *et al*. 2017, Bakr and Ahmad 2018, Liang *et al*. 2020a). Thus, the comparisons of the HS small model with the LE and EPP models are justifiable as the study aims to examine the accuracy of the LE and EPP models in simulating the seismic behaviour of shallow foundations.

2. Soil constitutive models

As mentioned in the introduction, three different soil constitutive models have been used to address the aim of this paper. These models were: the simple linear elasticity (LE) model, the Mohr-Coulomb elastic-perfectly-plastic (EPP) model, and the hardening soil with small strain stiffness (HS small) model. The reason to choose these models was, as mentioned before, to compare the performance of the models which have not been verified to work properly under the seismic loads (the LE and EPP models), with the HS small model, which has been shown to produce very good predictions to the response of the soil-structure interaction problems due to seismic loads; the verification of the HS small model can be found in Al-Defae *et al*. (2013), Amorosi *et al*. (2014), Liang *et al*. (2015), Knappett *et al*. (2015), Fabozzi and Bilotta (2016), Bakr and Ahmad (2018). Furthermore, these models are available in the commercial finite element software PLAXIS (Brinkgreve 2006); hence, it is practical to compare the behaviour of these models as the designers/researchers are expected to use one of these models.

The LE model is defined by two parameters; these parameters are the elasticity modulus (E) and the Poisson's ratio (υ) (Brinkgreve 2005). However, there is no definition to the failure in this model and the stress is linearly proportion to the applied stress depending on the E value. The EPP model is a bilinear model defined by five input parameters: the elasticity modulus (E), the Poisson's ratio (υ), the angle of internal friction (ϕ'), the cohesion (c'), and the dilatancy angle (ψ') (Ardakani *et al*. 2014). The elastic parameters control the settlement before reaching failure, while the shear strength parameters (ϕ' and c') control the failure conditions. Finally, the dilatancy angle (ψ') controls the irreversible volume change due to shearing for the non-associated flow rule conditions (Brinkgreve 2005).

The HS small model has been developed to accurately represent the dry soil in the finite element analysis; where this model captures the effect of the confining pressure and deviatoric stress on the soil stiffness, irrecoverable deformation of the soil, shear modulus degradation, and higher soil shear modulus at small strain stiffness. Benz (2007) developed this soil constitutive model utilizing the formulation of a model called the hardening soil model established by Schanz *et al*. (1999). However, it should be noted that the parameters of this soil model is relatively huge compared with the LE or the EPP models; these parameters are E_{50}^{ref}, E_{oed}^{ref}, E_{ur}^{ref}, P^{ref}, ϕ', c', ψ', υ_{ur}, m, R_f, K_O^{nc}, G_o^{ref}, and $\gamma_{0.7}$.

The triaxial reference stiffness (E_{50}^{ref}), the oedometer reference stiffness (E_{oed}^{ref}), and the unloading reference stiffness (E_{ur}^{ref}) are used in the model to calculate the soil stiffness considering different loading/unloading conditions. It is also necessary to mention that these stiffness parameters can be derived at any stress, which is called the reference stress P^{ref} (usually 100 kPa). The parameter m is utilized in the model to calculate the soil stiffness at any stress level. Furthermore, the model uses the classical shear strength parameters (ϕ' and c') to judge the failure conditions (i.e., the model utilizes the Mohr-Coulomb failure criteria). In additions, the volume change of the soil is modelled utilizing the dilatancy angle (ψ'). The parameter υ_u is used to specify the Poisson's ratio of the soil at unloading reloading stages. Moreover, the strain level at failure is specified using the parameter Rf, which is called the failure ratio. The soil lateral earth pressure in this model is calculated using the parameter K_O^{nc}.

Importantly, the shear modulus at small strain stiffness is specified in the HS small model using the parameter G_o^{ref}, which is called the reference small strain shear modulus, while the degradation of the soil shear/stiffness modulus is considered in this model using the strain level parameter ($\gamma_{0.7}$); this parameter is defined as the level of strain at which the secant shear modulus (G) drops to 70% of G_o^{ref}. The presence of the parameter $\gamma_{0.7}$ made the HS small model capable of considering the influence of the seismic effect on the stiffness of the soil, which is usually referred to as the stiffness degradation (Fabozzi *et al.* 2017; Obrzud 2017). The hysteresis damping is implicitly modeled in the HS small model because this model accurately simulates the soil hysteresis when subjected to cyclic loads (Brinkgreve *et al*. 2007). However, the model also requires considering the Rayleigh damping parameters (α and β) to consider the damping at small strain level (Brinkgreve *et al*. 2007, Bakr and Ahmed 2018). The readers are advised to read Benz (2007) and Benz *et al.* (2009) for further details on the model formulation. Also, useful information on the determination of most of the parameters of the model can be found in Bagbag *et al*. (2017) and Wu and Tung (2019).

3. Soil parameters

Silica sand with relative densities of 45% and 70% have been considered to address the aim of the study; Table 1

shows the HS small model parameters of these soils. These parameters have been calibrated by Al-Defae *et al*. (2013) based on the results of centrifuge modelling of a granular slope subjected to seismic shake. Moreover, these parameters have been successfully used to replicate the results of centrifuge modelling of two nearby buildings subjected to seismic shake (Knappett *et al*. 2015) and rooted slope subjected to earthquake excitation (Liang *et al*. 2015, 2020a, b). These parameters have also been used in previous studies on the modelling of the seismic response of buried tunnel (Kampas *et al*. 2019, Kampas *et al*. 2020). Rayleigh damping parameters (α and β) have also been considered for the analyses with the HS small model as the model does not accurately simulates the hysteretic damping at small strain level (Bakr and Ahmed 2018, 2019) and also to enhance the accuracy of the time history analysis (Forcellini 2019; 2020a, b). α and β values have been considered equal to 0.0005 and 0.005; these values have also been calibrated by Al-Defae *et al*. (2013). Figs. 1 and 2 show the tangent shear modulus (*Gt*) degradation, secant shear modulus (*Gs*) degradation, and damping ratio curves for relative density (DR) of 45% and 70%, respectively.

The analyses using the LE and EPP models have been conducted utilizing a modulus of elasticity increasing linearly with depth to provide more realistic conditions for these two simple models and to consider the best approach possible for these models (Yang *et al*. 2013). This has been done by calculating the modulus of elasticity at a depth of 0.1 m and at a depth of 40.0 m utilizing Equation 1 (Obrzud 2015, Zakhem and El Naggar 2019). The modulus of elasticity at a depth of 0.1 m has been considered as the reference modulus of elasticity (E_{ref}) and the rate of increase of the modulus of elasticity with depth ($E_{increase}$) has been calculated by subtracting the value of the modulus of elasticity at a depth of 0.1 m from the value of the modulus of elasticity at a depth of 40.0 m and dividing the result by 39.9 to find the rate of increase of the modulus of elasticity for every meter depth.

Table 2 shows the values of the E_{ref}, $E_{increase}$, and other soil parameters which are required to conduct LE and EPP analyses for DR 45% and 70%. It is clear from Table 2 that a Poisson's ratio value of 0.3 has been employed for both relative densities in the LE and EPP finite element analyses; this value is common for sand when conducting LE and EPP analyses (Fattah *et al*. 2015, Alzabeebee *et al*. 2018a, b, Zevgolis 2018, Alagha and Chapman 2019, Ekbote and Nainegali 2019a, b). Moreover, the same Rayleigh damping parameters (α = 0.0005 and β = 0.005) have been considered for the LE and EPP analyses to compensate for the lack of the hysteretic damping consideration in these soil models; similar approach has also been considered by Kampas *et al*. (2018).

$$E = 2(1+\upsilon)G_O \tag{1}$$

$$G_O(\sigma_3') = G_o^{ref}\left(\frac{c'\cot\phi' + \sigma_3'}{c'\cot\phi' + P_{ref}}\right)^m \tag{2}$$

$$\sigma_3' = K_O^{nc}\ \gamma\ H \tag{3}$$

where, σ_3' is the lateral earth pressure; and H is the depth of the soil.

Table 1 HS small model parameters (Al-Defae *et al*. 2013, Knappett *et al*. 2015)

Parameter	DR 45%	DR 70%
γ (kN/m^3)	15.85	16.60
E_{50}^{ref} (kPa)	39,338	47,150
E_{oed}^{ref} (kPa)	31,470	37,720
E_{ur}^{ref} (kPa)	94,410	113,160
G_o^{ref} (kPa)	111,300	123,800
$\gamma_{0.7}$	0.00014	0.00018
ϕ' (°)	38	43
ψ' (°)	7.25	13.50
c' (kPa)	0.1	0.1
m	0.555	0.530
R_f	0.9	0.9
υ_{ur}	0.2	0.2
p_{ref}	100	100

Table 2 LE and EPP model parameters

Parameter	DR 45%	DR 70%
γ (kN/m^3)	15.85	16.60
E_{ref} (kPa)	15,740	18,440
$E_{increase}$ (kPa)	10,550	10,580
υ_{ur}	0.3	0.3
ϕ' (°)	38	43
ψ' (°)	7.25	13.50
c' (kPa)	0.1	0.1

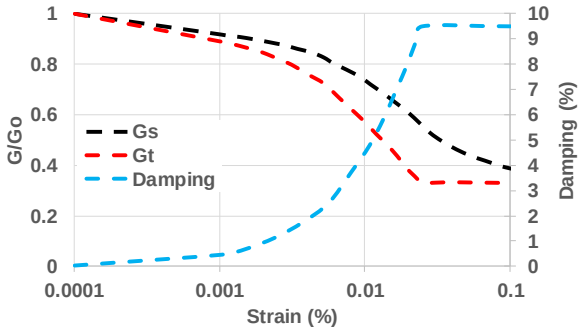

Fig. 1 Tangent shear modulus (*Gt*) degradation, secant shear modulus (*Gs*) degradation, and damping ratio curves for DR 45%

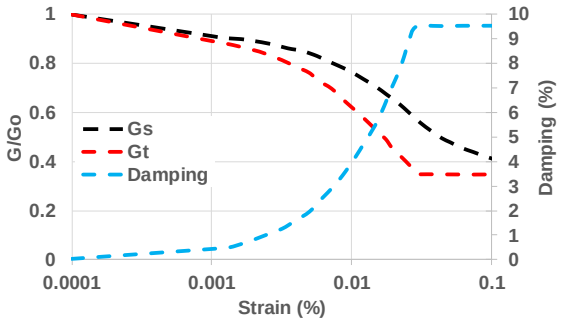

Fig. 2 Tangent shear modulus (*Gt*) degradation, secant shear modulus (*Gs*) degradation, and damping ratio curves for DR 70%

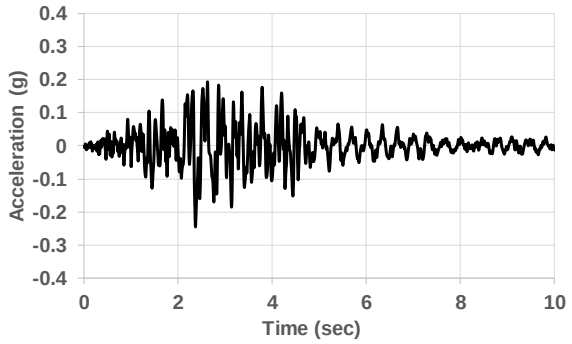

Fig. 3 Acceleration-time record of the Upland 1990 earthquake (Brinkgreve 2006)

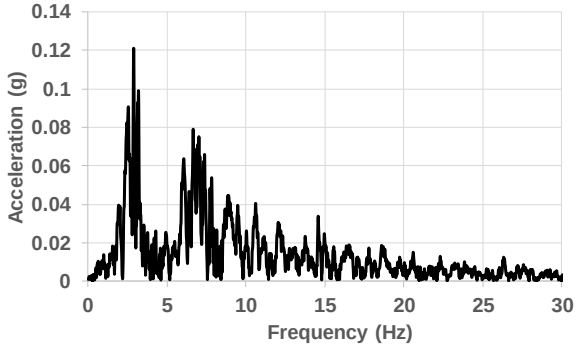

Fig. 4 Fourier transformation of the Upland 1990 earthquake record (Alzabeebee 2019a, b)

4. Earthquake record

The record of the upland earthquake shake is utilized in this research. Fig. 3 shows the time-acceleration record of this earthquake (Brinkgreve *et al.* 2006), while Fig. 4 shows the results of the Fourier transformation analysis, which has been conducted using SeismoSignal software. It is clear from both figures that this earthquake has a peak ground acceleration (PGA) of 0.24 g and dominant frequencies of 2.60 Hz and 6.70 Hz, respectively (Alzabeebee 2019a, b).

5. Numerical modelling of the problem

PLAXIS 2D has been used in the numerical modelling of the problem. A plane strain analysis has been conducted for the case of the strip foundation. The analysis involved static and dynamic stages as will be explained later in this section. The boundary conditions for the static analysis stage has been applied similar to previous studies (Alzabeebee *et al*. 2017, Acharyya and Dey 2018, Chavda and Dodagoudar 2018, 2019, Kadivar *et al*. 2018, Ouahab *et al*. 2018, 2020, Zevgolis 2018, Alzabeebee *et al*. 2018a, b, 2019a, b, Ekbote and Nainegali 2019a, b), where the bottom of the mesh has been fixed against the movement in all directions to consider the influence of the undeformed rock layer and the left- and right-hand sides of the model have been allowed to move only in the vertical direction. Moreover, the absorbent boundaries have been considered in the dynamic analysis stage to eliminate the influence of the wave reflection back to the finite element model during the time-history finite element analysis (Fattah *et al*. 2015, Alzabeebee 2019a, b, Meena and Nimbalkar 2019, Alzabeebee 2020a, b, c, Forcellini 2020b, Mina and Forcellini 2020). These absorbent boundaries have been added to the left and right sides of the model boundaries.

The depth of the numerical model has been considered equal to 40 m because the location of the rock layer has been assumed to be at a depth of 40 m from the natural ground surface; similar modelling approach has been used in other studies in the literature (Nguyen *et al*. 2016, Alzabeebee 2019a, b). The width of the model has been considered equal to 80 m. This width has been chosen based on parametric analyses conducted to investigating the influence of the finite element model width. The parametric analyses have been done by simulating different model widths and selecting the width after which there is no influence of the finite element model extend on results of the analysis. The results of the model width study are shown in Fig. 5, which clearly shows that the model width has an insignificant influence on the obtained results and this influence is diminished after a model width of 80 m. It is important to mention that the results in Fig. 5 have been obtained using the HS small model and for sandy soil with a relative density of 45%.

15-node solid elements with 12 stress points have been used to model the soil. In addition, the foundation has been modelled as a rigid concrete block using the same solid elements (15-node elements). Furthermore, linear elastic model has been employed to model the response of the foundation.

The mesh size has also been selected after conducting mesh convergence study to ensure that the obtained results are independent of the mesh size. The results of the mesh convergence study are shown in Fig. 6 (also using HS small model and for a relative density of 45%). The results of Fig. 6 shows that the number of elements has an unpronounced effect on the obtained results and this effect becomes almost unnoticeable when the number of elements becomes equal to 2568 element; hence, this number of elements have been selected in this study.

The earthquake has been simulated as a prescribed acceleration applied at the bottom of the finite element model (which is the location of the rock layer); this approach is common in simulating the effect of the earthquake in the finite element analysis (Bhatnaga *et al.* 2016, Kholdebarin *et al*. 2016, Alzabeebee 2019a, b, Dhar *et al*. 2019, Fatahi *et al*. 2019, Karalar and Cavusli 2019, Roy *et al*. 2019, Tsinidis *et al*. 2019). The finite element mesh of the problem is shown in Fig. 7. The LE model has been employed to simulate the response of the foundation; the E and υ values of the concrete foundation have been considered equal to 25,000,000 kPa and 0.2, respectively similar to a previous study by the author (Alzabeebee 2019b). A surface static load has been applied on the foundation in the static stage to simulate the pressure applied from a residential building; the value of the load has been considered equal to 150 kPa based on the study of Maheshwari and Viladkar (2007). The analysis of the developed model involved three stage as follows:

- The first stage concerned with the calculation of the initial stresses of the soil. These initial stresses have been

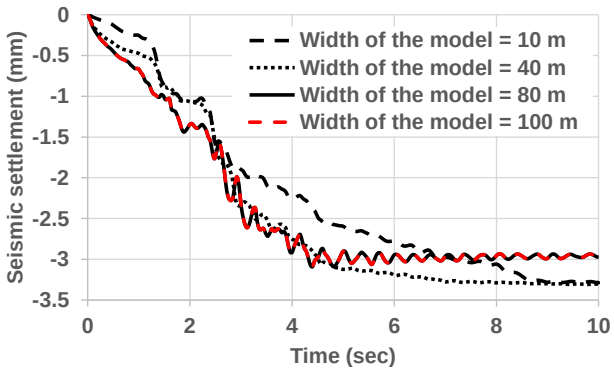

Fig. 5 Results of the parametric study of the effect of the finite element model extent for a foundation resting on sandy soil with a relative density of 45%

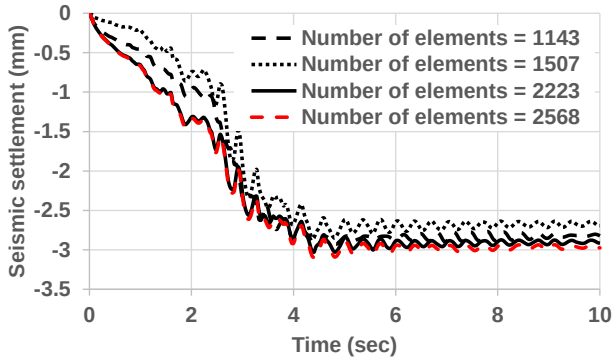

Fig. 6 Results of the mesh sensitivity study for a foundation resting on sandy soil with a relative density of 45%

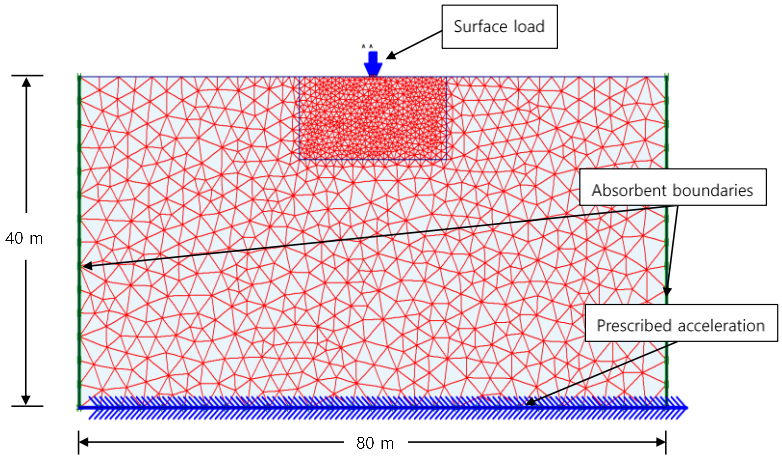

Fig. 7 The finite element mesh of the shallow foundation

calculated by utilizing the soil unit weight and the at-rest coefficient of earth pressure.

- The second stage concerned with the application of the surface load on the foundation (which is 150 kPa as mentioned earlier).

- The third stage concerned with conducting the time-history finite element analysis. This has been achieved by activating the absorbent boundaries and the earthquake at the bottom of the model. The time-step used in the analysis is equal to 0.0004 Sec to allow accurate modelling (Alzabeebee 2019a, b). The time step satisfies the Courant-Friedrichs-Lewy condition as it has been determined based on the wavelength and the mesh height as suggested by Alzabeebee *et al.* (2018a).

6. Results of the analyses

6.1 Analyses using the upland earthquake

Figs. 8 and 9 compare the results of the seismic settlement obtained using the LE, EPP, and HS small models for DR 45% and 70%, respectively. The results in Figs. 8 and 9 have been obtained using the original

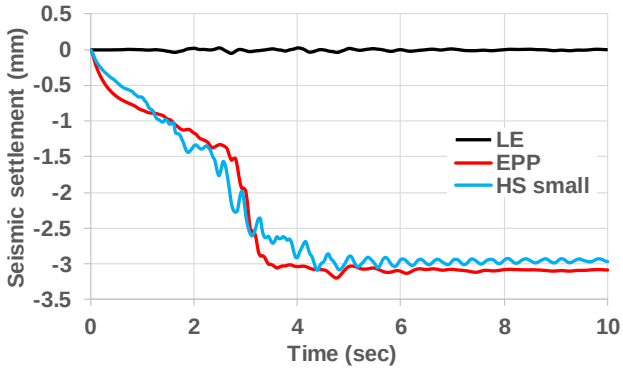

Fig. 8 Influence of the soil model on the seismic settlement of the foundation for the case of DR 45%

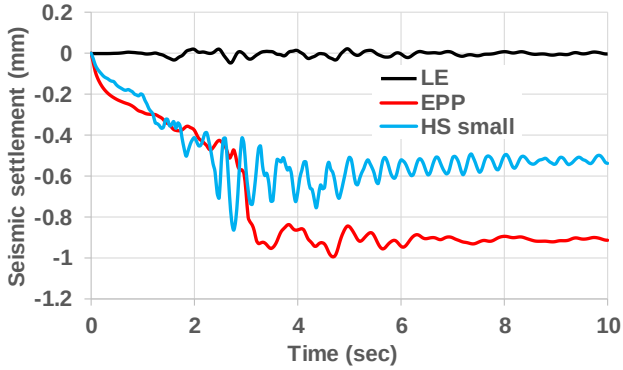

Fig. 9 Influence of the soil model on the seismic settlement of the foundation for the case of DR 70%

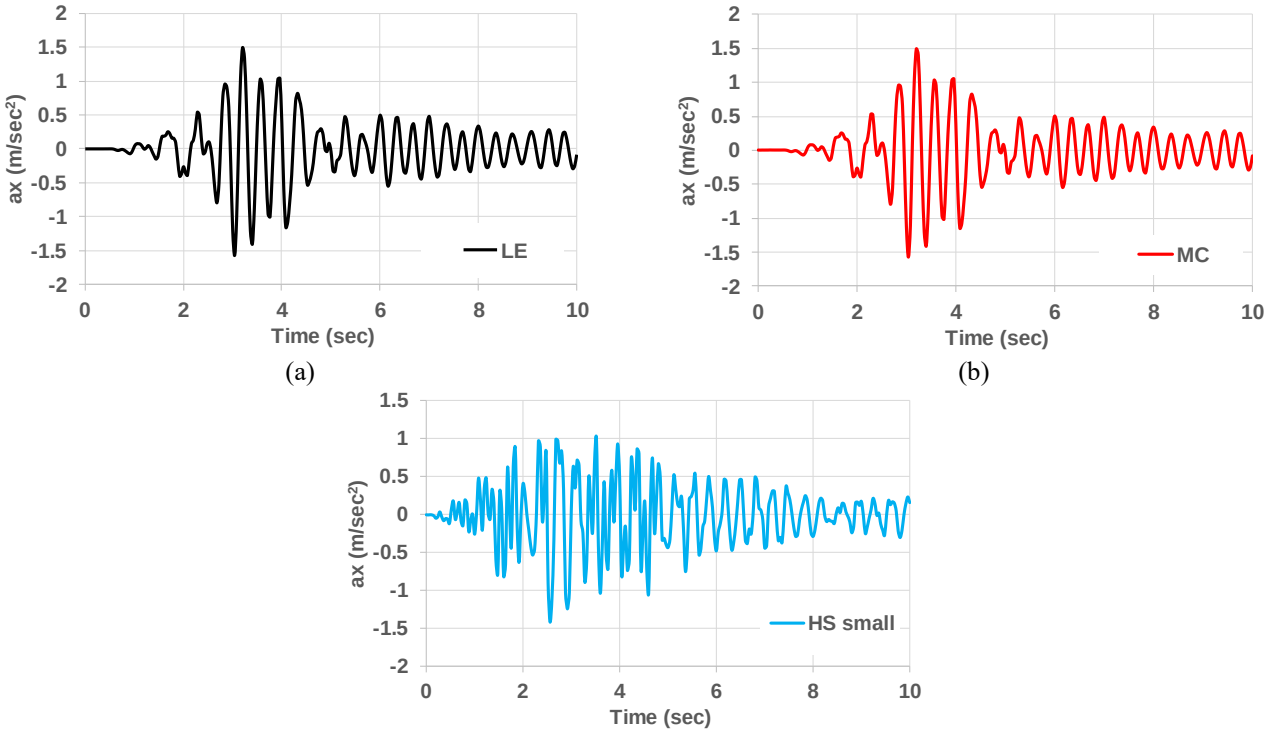

Fig. 10 Acceleration developed beneath the foundation for the case of DR 45%: (a) analysis using LE model, (b) analysis using EPP model and (c) analysis using HS small model

earthquake record shown in Fig. 3 with a PGA of 0.24 g. It is also important to mentioned that only the seismic settlement has been presented in the figures and this is why the settlement starts from zero in these figures (i.e., the

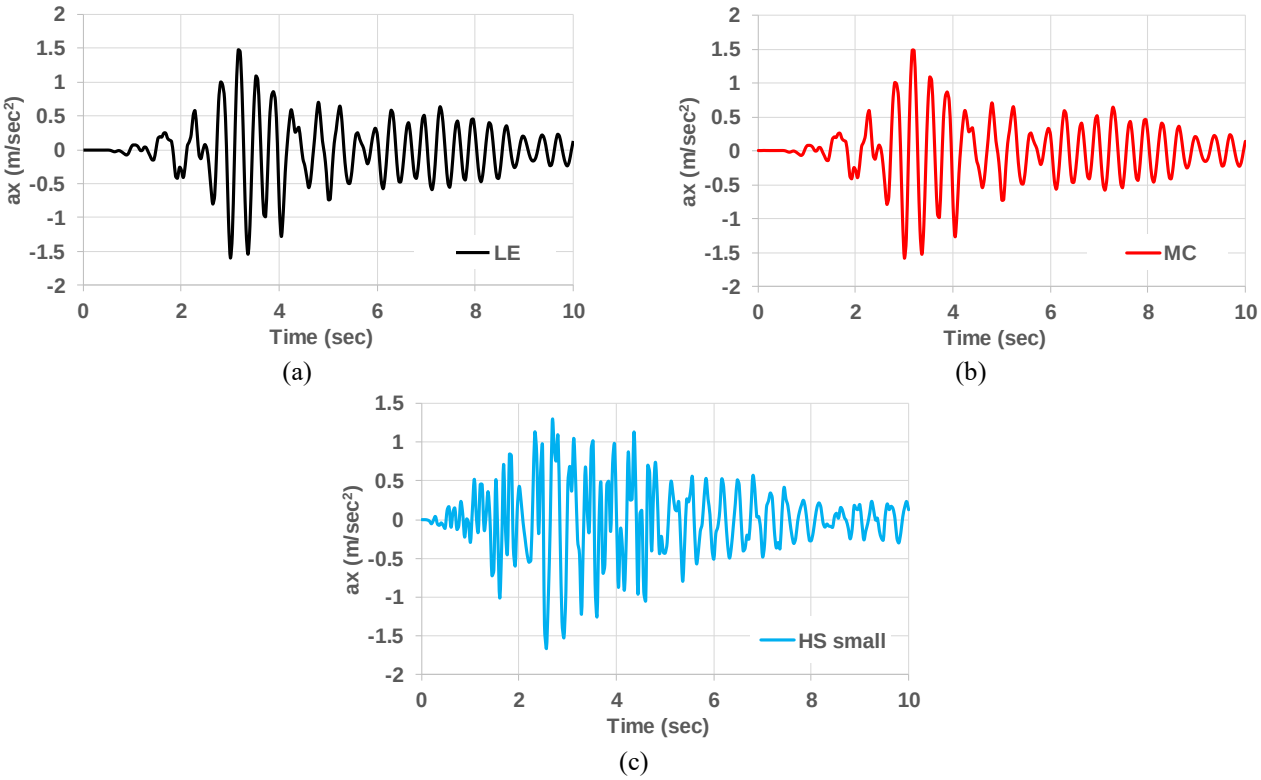

Fig. 11 Acceleration developed beneath the foundation for the case of DR 45%: (a) analysis using LE model, (b) analysis using EPP model and (c) analysis using HS small model

static settlement has been subtracted from the total settlement to obtain the seismic settlement before drawing these figures). This has been done to clearly present the influence of the soil model on the seismic settlement. The figures clearly show that the seismic settlement produced using the LE model is very small and almost equal to zero regardless of the relative density of the soil. However, the settlement produced utilizing the EPP model increases in stages until reaching a stabilized value at a time of about 3.6 Sec for DR 45% and 6.4 Sec for DR 70%. This staged increase of the seismic settlement is due to the change of the acceleration as the EPP model is sensitive to the change of the acceleration and produces an increase in the settlement when the acceleration remarkably rises. On the other hand, the figures show that the HS small model produces almost the same trend and magnitude as the EPP model for the case of DR 45%. However, the results of DR 70% show that the HS small model produces seismic settlement lower than the EPP model and also the trend of the seismic settlement with time is different, where the Hs small model shows a decrease in the settlement after a time value of 4.4 Sec and then the settlement stabilizes at approximately 8.5 Sec. This decrease of the seismic settlement is due to the additional compaction provided to the soil as the cycles of the earthquake increases, which can be captured in the HS small model (Alzabeebee 2019a).

Figs. 10 and 11 present the acceleration developed directly underneath the foundation obtained using the LE, EPP, and HS small models for DR 45% and 70%, respectively. The results clearly show that the trend and magnitude of the acceleration-time relationship is similar for the LE and EPP models. This behaviour is because both models utilize a constant stiffness, which is independent of the stress and strain level of the soil. However, the trend of the acceleration-time relationship obtained using the HS small model is different than the LE and EPP model, which is expected as the soil stiffness in the HS small model changes with the change of the stress level and also due to shear modulus degradation.

6.2 Effect of the PGA

The effect of the PGA value of the earthquake shake on the results of the soil models has also been investigated in this study; this has been done by scaling the Upland earthquake to produced new earthquake records with a PGA value range of 0.1 g to 1.0 g. The scaling procedure is similar to that used in previous studies (Abuhajar *et al.* 2015a, b, Bakr and Ahmed 2018). These new records have been used in different analyses to determine the seismic settlement.

Fig. 12 shows the relationship between the PGA value and the maximum seismic settlement (SS) obtained using the LE, EPP, and HS small models for the case of DR 45%. It is clear from the figure that the LE model produces very small seismic settlement (almost equal to zero) regardless of the PGA value of the earthquake. However, the interesting finding is that the EPP model produces a seismic settlement higher than the HS small model for cases with a PGA value lower 0.25 g. However, after a PGA value of 0.25 g, the HS small model produces higher seismic settlement with the difference between the HS small and EPP models increases

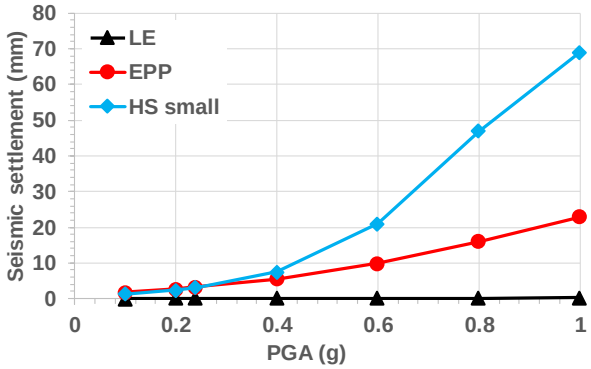

Fig. 12 Effect of the PGA and soil constitutive model on the maximum seismic settlement for foundation resting on sandy soil with DR 45%

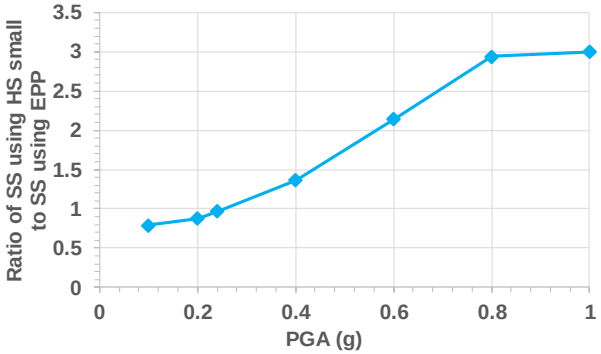

Fig. 13 Ratio of the maximum seismic settlement (SS) obtained using the HS small model to the SS obtained using the EPP model for the case of DR 45%

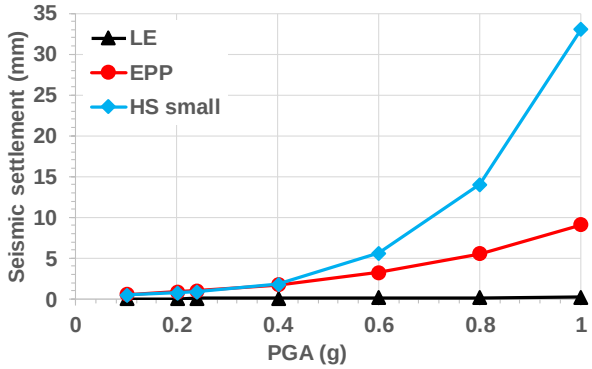

Fig. 14 Effect of the PGA and soil constitutive model on the maximum seismic settlement for foundation resting on sandy soil with DR 70%

as the PGA value rises. This can be clearly seen in Fig. 13, which presents the relationship between the PGA value and the ratio of the maximum seismic settlement (SS) obtained using the HS small model to that obtained using the EPP model. It is obvious from Fig. 13 that the ratio has a non-linear trend and increases as the PGA value rises, starting from a value of 0.80 until reaching a maximum value of 3.00. This behaviour is due to the significant decline of the soil stiffness as the PGA value increases; the decrease of the stiffness remarkably rises the seismic settlement and makes the HS small model produces SS remarkably higher than that obtained using the EPP model, which utilizes a constant

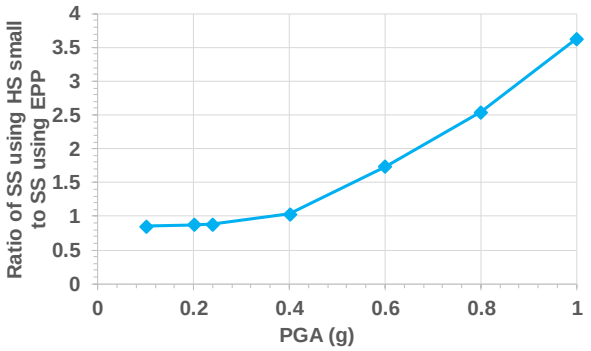

Fig. 15 Ratio of the maximum seismic settlement (SS) obtained using the HS small model to the SS obtained using the EPP model for the case of DR 70%

stiffness. Importantly, the results of Fig. 13 indicate that the EPP model can be used in the analyses of the seismic response of shallow foundation within a limited PGA range.

Fig. 14 presents the relationship between the maximum seismic settlement and the PGA value for the case of DR 70%. The figure shows similar trend to that already discussed for the case of DR 45%, where the LE model produces very small seismic settlement compared with the EPP and HS small models. The figure also shows that, similar to the case of DR 45%, the EPP model produces seismic settlement higher than the HS small model. However, the difference between both models decreases as the PGA value rises until the seismic settlement obtained using the HS small model becomes higher than that produced using the EPP model when the PGA value rises above 0.40 g. Again, this behaviour is attributed to the decrease of the soil stiffness as the PGA value increases for the case of the HS small model; the decrease of the stiffness gradually reduces the difference between both models and then makes the HS small model produces settlement higher than the EPP model. Fig. 15 shows the ratio of the maximum seismic settlement (SS) obtained using the HS small model to the seismic settlement obtained using the EPP model. The results of the figure clearly show that the ratio ranges between 0.85 to 3.62 with a value of 1.0 (i.e., both models produce the same seismic settlement) for the case of a PGA value of 0.40 g.

Based on these comparisons, it can be concluded that the use of the EPP model may provide inaccurate results and underestimates the seismic settlement for earthquakes with high PGA values, where the maximum underestimation percentage reaches 300% and 350% for relative densities of 45% and 70%, respectively; such percentage is very high and even a factor of safety cannot compensate it. However, the results of the analyses also demonstrated the applicability of using the EPP model as a conservative solution for earthquakes with PGA lower than or equal to 0.24 g for the case of DR 45% and 0.39 g for the case of DR 70%. This finding is very important because the EPP model is not computationally demanding compared with the HS small model, where the analysis time was approximately 30 minutes for the simulation utilizing EPP model, while the analysis time was approximately 180 minutes for the same simulation but with the HS small

model. Furthermore, the LE model should not be used to analyze the seismic soil-foundation interaction as the results showed that this model produced a very small seismic settlement regardless of the relative density of the soil.

7. Conclusions

This research examined the effect of the sophistication of the soil constitutive relationship on the accuracy of the finite element analysis of a shallow foundation subjected to seismic shake. The aim of the research has been achieved by comparing the results of the linear elastic (LE) model and the elastic perfectly plastic (EPP) model with the results of the hardening soil with a small-strain stiffness (Hs small) model, which is a model accurately replicates the behaviour of soil-structure interaction problems subjected to seismic effects as has been demonstrated by numerous research studies (Al-Defae *et al*. 2013, Amorosi *et al*. 2014, Liang *et al*. 2015, Knappett *et al*. 2015, Fabozzi and Bilotta 2016, Amorosi *et al*. 2017, Bakr and Ahmad 2018 and Liang *et al*. 2020a). In addition, sandy soil with two relative densities (45% and 70%) have been employed to examine the influence of the soil model. The study commenced with a brief description of the aforementioned soil models; then, the three models have been used to analyze the behaviour of a shallow foundation subjected to seismic shake. The following brief the unique conclusions of the study:

- The LE model produces almost zero seismic settlement compared with the EPP and HS small models regardless of the relative density of the sandy soil.

- The EPP and HS small models show similar trend of the seismic settlement with time for the case of a relative density of 45%. However, the trend was different for the relative density of 70%, where the EPP model failed to simulate the slight decrease of the seismic settlement due to the densification of the stiff soil as the intensity of the seismic shake increased.

- The EPP model produces settlement higher than the HS small model for a PGA value less than 0.25 g for the case of a relative density of 45% and a PGA value less than 0.40 g for a relative density of 70%. This means that the EPP model can be used with confidence as a conservative solution for studying the behaviour of shallow foundations subjected to earthquakes with a PGA value lower than the those stated earlier; however, further studies with different earthquake records are required to provide more broad insight into this point. Nevertheless, this finding is very important as this model is not computationally demanding compared with the HS small model.

- The HS small model gives seismic settlement values higher than the EPP model for a PGA value greater than 0.25 g and 0.40 g for a relative density of 45% and 70%, respectively. In addition, the difference between the two models increases as the PGA value rises; this is due to the dramatic decrease of the soil stiffness caused by stiffness degradation as the PGA value rises.

- Increasing the relative density (i.e., stiffness) of the soil rises the PGA value beyond which the EPP model starts to underestimate the seismic settlement. This is due to the decrease of the influence of stiffness degradation as the relative density (stiffness) surges.

- The LE and EPP models produce the same trend and magnitudes of the acceleration-time relationship directly below the foundation, while the trend of the same relationship obtained using the HS small model is different. This is due to the change of the stiffness with time for the case of the HS small model.

References

Abuhajar, O., El Naggar, H. and Newson, T. (2015a), "Seismic soil-culvert interaction", *Can. Geotech. J.*, **52**(11), 1649-1667. https://doi.org/10.1139/cgj-2014-0494.

Abuhajar, O., El Naggar, H. and Newson, T. (2015b), "Experimental and numerical investigations of the effect of buried box culverts on earthquake excitation", *Soil Dyn. Earthq. Eng.*, **79**, 130-148. https://doi.org/10.1016/j.soildyn.2015.07.015.

Acharyya, R. and Dey, A. (2018), "Assessment of failure mechanism of a strip footing on horizontal ground considering flow rules", *Innov. Infrastruct. Solut.*, **3**(1), 49. https://doi.org/10.1007/s41062-018-0150-7.

Al-Defae, A.H. Caucis, K. and Knappett, J.A. (2013), "Aftershocks and the whole-life seismic performance of granular slopes", *Géotechnique*, **63**(14), 1230-1244. https://doi.org/10.1680/geot.12.P.149.

Alagha, A.S. and Chapman, D.N. (2019), "Numerical modelling of tunnel face stability in homogeneous and layered soft ground", *Tunn. Undergr. Sp. Tech.*, **94**, 103096. https://doi.org/10.1016/j.tust.2019.103096.

Alzabeebee, S. (2019a), "Response of buried uPVC pipes subjected to earthquake shake", *Innov. Infrastruct. Solut.*, **4**(1), 52. https://doi.org/10.1007/s41062-019-0243-y.

Alzabeebee, S. (2019b), "Seismic response and design of buried concrete pipes subjected to soil loads", *Tunn. Undergr. Sp. Tech.*, **93**, 103084. https://doi.org/10.1016/j.tust.2019.103084.

Alzabeebee, S., (2020a), "Seismic settlement of a strip foundation resting on a dry sand", *Nat. Hazards*, **103**, 2395-2425. https://doi.org/10.1007/s11069-020-04090-w.

Alzabeebee, S. (2020b), "Dynamic response and design of a skirted strip foundation subjected to vertical vibration", *Geomech. Eng.*, **20**(4), 345-358. http://doi.org/10.12989/gae.2020.20.4.345.

Alzabeebee, S. (2020c), "Numerical analysis of the interference of two active machine foundations", *Geotech. Geol. Eng.*, **38**, 5043-5059. https://doi.org/10.1007/s10706-020-01347-w.

Alzabeebee, S., Chapman, D.N. and Faramarzi, A., (2017), "Numerical investigation of the bedding factor of concrete pipes under deep soil fill", *Proceedings of the 2nd World Congress on Civil, Structural, and Environmental Engineering (CSEE'17)*, Barcelona, Spain, April.

Alzabeebee, S., Chapman, D.N. and Faramarzi, A. (2018a), "A comparative study of the response of buried pipes under static and moving loads", *Transport. Geotech.*, **15**, 39-46. https://doi.org/10.1016/j.trgeo.2018.03.001.

Alzabeebee, S., Chapman, D.N. and Faramarzi, A. (2018b), "Innovative approach to determine the minimum wall thickness of flexible buried pipes", *Geomech. Eng.*, **15**(2), 755-767. http://doi.org/10.12989/gae.2018.15.2.755.

Amorosi, A., Boldini, D. and Falcone, G. (2014), "Numerical prediction of tunnel performance during centrifuge dynamic tests", *Acta Geotechnica*, **9**(4), 581-596. https://doi.org/10.1007/s11440-013-0295-7.

Amorosi, A., Boldini, D. and Lernia, A. (2017), "Dynamic soil-

structure interaction: A three-dimensional numerical approach and its application to the Lotung case study", *Comput. Geotech.*, **90**, 34-54. https://doi.org/10.1016/j.compgeo.2017.05.016.

Ardakani, A., Bayat, M. and Javanmard, M. (2014), "Numerical modeling of soil nail walls considering Mohr Coulomb, hardening soil and hardening soil with small strain stiffness effect models", *Geomech. Eng.*, **6**(4), 391-401. http://doi.org/10.12989/gae.2014.6.4.391.

Bagbag, A.A., Lehane, B.M. and Doherty, J.P. (2017), "Predictions of footing and pressuremeter response in sand using a hardening soil model", *Proc. Inst. Civ. Eng. Geotech. Eng.*, **170**(6), 479-492. https://doi.org/10.1680/jgeen.17.00040.

Bakr, J. and Ahmad, S.M. (2018), "A finite element performance-based approach to correlate movement of a rigid retaining wall with seismic earth pressure", *Soil Dyn. Earthq. Eng.*, **114**, 460-479. https://doi.org/10.1016/j.soildyn.2018.07.025.

Bakr, J., Ahmad, S.M. and Lombardi, D. (2019), "Finite-element study for seismic structural and global stability of cantilever-type retaining walls", *Int. J. Geomech.*, **19**(10), 04019117. https://doi.org/10.1061/(ASCE)GM.1943-5622.0001505.

Benz, T. (2007), "Small-strain stiffness of soils and its numerical consequences", Ph.D. Thesis, University of Stuttgart, Sttugart, Germany.

Benz, T., Schwab, R. and Vermeer, P. (2009) "Small-strain stiffness in geotechnical analyses", *Bautechnik*, **86**(S1), 16-27. https://doi.org/10.1002/bate.200910038.

Bhatnagar, S., Kranthikumar, A. and Sawant, V.A. (2016) "Seismic analysis of dam under different upstream water levels", *Adv. Comput. Des.*, **1**(3), 265-274. https://doi.org/10.12989/acd.2016.1.3.265.

Brinkgreve R.B.J., Kappert M.H. and Bonnier, P.G. (2007), "Hysteretic damping in a small-strain stiffness model", *Proceeding of the Numerical Models in Geomechanics*, NUMOG X, Rhodes, Greece, April.

Brinkgreve, R.B., (2005), "Selection of soil models and parameters for geotechnical engineering application", *Proceedings of the Geo-Frontiers Congress 2005*, Austin, Texas, U.S.A., January.

Brinkgreve, R.B.J., Broere, W. and Waterman, D. (2006), *Finite Element Code for Soil and Rock Analyses Users Manual*, Plaxis, The Netherlands.

Brinkgreve, R.B.J., Engin, E. and Engin, H.K. (2010), *Validation of Empirical Formulas to Derive Model Parameters for Sands*, in *Numerical Methods in Geotechnical Engineering*, CRC Press, Rotterdam, The Netherlands.

Chavda, J.T. and Dodagoudar, G.R. (2018), "Finite element evaluation of ultimate capacity of strip footing: Assessment using various constitutive models and sensitivity analysis", *Innov. Infrastruct. Solut.*, **3**(1), 15. https://doi.org/10.1007/s41062-017-0121-4.

Chavda, J.T. and Dodagoudar, G.R. (2019), "On vertical bearing capacity of ring footings: Finite element analysis, observations and recommendations", *Int. J. Geotech. Eng.*, 1-13. https://doi.org/10.1080/19386362.2019.1648737.

Dhar, S., Ozcebe, A.G., Dasgupta, K., Petrini, L. and Paolucci, R. (2019), "Different approaches for numerical modeling of seismic soil-structure interaction: Impacts on the seismic response of a simplified reinforced concrete integral bridge", *Earthq. Struct.*, **17**(4), 373-385. http://doi.org/10.12989/eas.2019.17.4.373.

Ekbote, A.G. and Nainegali, L. (2019a), "Interference of two closely spaced footings embedded in unreinforced and reinforced soil medium: A finite element approach using ABAQUS", *Arab. J. Geosci.*, **12**(22), 683. https://doi.org/10.1007/s12517-019-4868-0.

Ekbote, A.G. and Nainegali, L. (2019b), "Finite element analysis of two nearby interfering asymmetric footings embedded in cohesionless foundation medium", *Geomech. Geoeng.*, 1-14. https://doi.org/10.1080/17486025.2019.1664776.

Elshimi, T.M. and Moore, I.D. (2013), "Modeling the effects of backfilling and soil compaction beside shallow buried pipes", *J. Pipeline Syst. Eng. Pract.*, **4**(4), 04013004. https://doi.org/10.1061/(ASCE)PS.1949-1204.0000136.

Fabozzi, S., Licata, V., Autuori, S., Bilotta, E., Russo, G. and Silvestri, F. (2017), "Prediction of the seismic behavior of an underground railway station and a tunnel in Napoli (Italy)", *Undergr. Sp.*, **2**(2), 88-105. https://doi.org/10.1016/j.undsp.2017.03.005.

Fabozzi, S. and Bilotta, E. (2016), "Behaviour of a segmental tunnel lining under seismic actions", *Procedia Eng.*, **158**, 230-235. https://doi.org/10.1016/j.proeng.2016.08.434.

Fatahi, B., Huang, B., Yeganeh, N., Terzaghi, S. and Banerjee, S. (2019), "Three-dimensional simulation of seismic slope-foundation-structure interaction for buildings near shallow slopes", *Int. J. Geomech.*, **2**0(1), 04019140. https://doi.org/10.1061/(ASCE)GM.1943-5622.0001529.

Fattah, M.Y., Hamoo, M.J. and Dawood, S.H. (2015), "Dynamic response of a lined tunnel with transmitting boundaries", *Earthq. Struct.*, **8**(1), 275-304. http://doi.org/10.12989/eas.2015.8.5.275.

Forcellini, D. (2019), "Numerical simulations of liquefaction on an ordinary building during Italian (20 May 2012) earthquake", *B. Earthq. Eng.*, **17**(9), 4797-4823. https://doi.org/10.1007/s10518-019-00666-5.

Forcellini D (2020a), "Soil-structure interaction analyses of shallow-founded structures on a potential-liquefiable soil deposit", *Soil Dyn. Earthq. Eng.*, **133**, 106108. https://doi.org/10.1016/j.soildyn.2020.106108.

Forcellini, D. (2020b), "The role of the water level in the assessment of seismic vulnerability for the 23 November 1980 Irpinia-Basilicata earthquake", *Geosciences*, **10**(6), 229. https://doi.org/10.3390/geosciences10060229.

Kadivar, M., Manahiloh, K.N., Kaliakin, V.N. and Shenton, H.W. (2018), "Numerical investigation of dynamic load amplification in buried culverts", *Transport Infrastruct. Geotechnol.*, **5**(1), 24-41. https://doi.org/10.1007/s40515-017-0045-7.

Kampas, G., Knappett, J., Brown, M., Anastasopoulos, I., Fuentes, R., Nikitas, N. and Alonso-Rodriguez, A. (2018), "Suitability of equivalent linear soil models for analysing the seismic response of a concrete tunnel", *Proceedings of the 16th European Conference on Earthquake Engineering*, Thessaloniki, Greece, June.

Kampas, G., Knappett, J.A., Brown, M.J., Anastasopoulos, I., Nikitas, N. and Fuentes, R. (2020), "Implications of volume loss on the seismic response of tunnels in coarse-grained soils", *Tunn. Undergr. Sp. Tech.*, **95**, 103127. https://doi.org/10.1016/j.tust.2019.103127.

Kampas, G., Knappett, J.A., Brown, M.J., Anastasopoulos, I., Nikitas, N. and Fuentes, R. (2019), "The effect of tunnel lining modelling approaches on the seismic response of sprayed concrete tunnels in coarse-grained soils", *Soil Dyn. Earthq. Eng.*, **117**, 122-137. https://doi.org/10.1016/j.soildyn.2018.11.018.

Karalar, M. and Cavusli, M. (2019), "Assessing 3D seismic damage performance of a CFR dam considering various reservoir heights", *Earthq. Struct.*, **16**(2), 221-234. http://doi.org/10.12989/eas.2019.16.2.221.

Kholdebarin, A., Massumi, A. and Davoodi, M. (2016), "Seismic bearing capacity of shallow footings on cement-improved soils", *Earthq. Struct.*, **10**(1), 179-190. http://doi.org/10.12989/eas.2016.10.1.179,

Knappett, J.A., Madden, P. and Caucis, K. (2015), "Seismic structure-soil-structure interaction between pairs of adjacent building structures", *Géotechnique*, **65**(5), 429-441.

https://doi.org/10.1680/geot.SIP.14.P.059.
Kontoe, S., Zdravkovic, L., Potts, D.M. and Menkiti, C.O. (2011), "On the relative merits of simple and advanced constitutive models in dynamic analysis of tunnels", *Géotechnique*, **61**(10), 815-829. https://doi.org/10.1680/geot.9.P.141.
Liang, T., Knappett, J.A. and Duckett, N. (2015), "Modelling the seismic performance of rooted slopes from individual root-soil interaction to global slope behaviour", *Géotechnique*, **65**(12), 995-1009. https://doi.org/10.1680/jgeot.14.P.207.
Liang, T., Knappett, J.A., Leung, A., Carnaghan, A., Bengough, A.G. and Zhao, R. (2020b), "A critical evaluation of predictive models for rooted soil strength with application to predicting the seismic deformation of rooted slopes", *Landslides*, **17**(1), 93-109. https://doi.org/10.1007/s10346-019-01259-8.
Liang, T., Knappett, J.A., Leung, A.K. and Bengough, A.G. (2020a), "Modelling the seismic performance of root-reinforced slopes using the Finite Element Method", *Géotechnique*, **70**(5), 375-391. https://doi.org/10.1680/jgeot.17.P.128.
Maheshwari, P. and Viladkar, M.N. (2007), "Strip footings on a three layer soil system: Theory of elasticity approach", *Int. J. Geotech. Eng.*, **1**(1), 47-59. https://doi.org/10.3328/IJGE.2007.01.01.47-59.
Meena, N.K. and Nimbalkar, S. (2019), "Effect of water drawdown and dynamic loads on piled raft: Two-dimensional finite element approach", *Infrastructures*, **4**(4), 75. https://doi.org/10.3390/infrastructures4040075.
Mina, D. and Forcellini, D. (2020), "Soil-structure interaction assessment of the 23 November 1980 Irpinia-Basilicata Earthquake", *Geosciences*, **10**(4), 152. https://doi.org/10.3390/geosciences10040152.
Nguyen, Q.V., Fatahi, B. and Hokmabadi, A.S. (2016), "The effects of foundation size on the seismic performance of buildings considering the soil-foundation-structure interaction", *Struct. Eng. Mech.*, **58**(6), 1045-1075. http://doi.org/10.12989/sem.2016.58.6.1045.
Obrzud, R. (2015), C*onstitutive Models for Practice in ZSoil v2014*, Lausanne, Switzerland.
Ouahab, M.Y., Mabrouki, A., Frank, R., Mellas, M. and Benmeddour, D. (2020), "Undrained bearing capacity of strip footings under inclined load on non-homogeneous clay underlain by a rough rigid base", *Geotech. Geol. Eng.*, **38**(2), 1733-1745. https://doi.org/10.1007/s10706-019-01127-1.
Ouahab, M.Y., Mabrouki, A., Mellas, M. and Benmeddour, D. (2018), "Effect of load eccentricity on the bearing capacity of strip footings on non-homogenous clay overlying bedrock", *Transport. Infrastruct. Geotechnol.*, **5**(2), 169-186. https://doi.org/10.1007/s40515-018-0055-0.
Roy, N., Bharti S.D. and Kumar, A. (2019), "Seismic isolation of tunnels in blocky rock mass using expanded polystyrene (EPS) Geofoam", *Innov. Infrastruct. Solut.*, **4**(1), 38. https://doi.org/10.1007/s41062-019-0225-0.
Schanz, T., Vermeer, P.A. and Bonnier, P.G. (1999), *The Hardening Soil Model: Formulation and Verification*, in *Beyond 2000 in Computational Geotechnics*, CRC Press, Rotterdam, The Netherlands, 281-296.
Tsinidis, G., Papantou, M. and Mitoulis, S. (2019), "On the response of integral abutment bridges under a sequence of thermal loading and ground seismic shaking", *Earthq. Struct.*, **16**(1), 11-28. https://doi.org/10.12989/eas.2019.16.1.011.
Wu, J.T.H. and Tung, S.C.Y. (2020), "Determination of model parameters for the hardening soil model", *Transport. Infrastruct. Geotechnol.*, **7**(1), 55-68. https://doi.org/10.1007/s40515-019-00085-8.
Yang, W., Hussein, M.F.M., Marshall, A.M. and Cox, C. (2013), "Centrifuge and numerical modelling of ground borne vibration from surface sources", *Soil Dyn. Earthq. Eng.*, **44**, 78-89. https://doi.org/10.1016/j.soildyn.2012.09.003.
Yeganeh, N. and Fatahi, B. (2019), "Effects of choice of soil constitutive model on seismic performance of moment-resisting frames experiencing foundation rocking subjected to near-field earthquakes", *Soil Dyn. Earthq. Eng.*, **121**, 442-459. https://doi.org/10.1016/j.soildyn.2019.03.027.
Zakhem, A.M. and El Naggar, H. (2019), "Effect of the constitutive material model employed on predictions of the behaviour of earth pressure balance (EPB) shield-driven tunnels", *Transport. Geotech.*, **21**, 100264. https://doi.org/10.1016/j.trgeo.2019.100264.
Zevgolis, I.E. (2018), "A finite element investigation on displacements of reinforced soil walls under the effect of typical traffic loads", *Transport. Infrastruct. Geotechnol.*, **5**(3), 231-249. https://doi.org/10.1007/s40515-018-0059-9.

IC